Journal of Biomedical Optics 6(2), 111–115 (April 2001)

Recognition of hypermethylated triplet repeats *in vitro* by cationic nanoparticles

Latha Gearheart
K. K. Caswell
Catherine J. Murphy
University of South Carolina
Department of Chemistry and Biochemistry
631 Sumter Street
Columbia, South Carolina 29208

Abstract. Genomic DNA contains many higher-order structural deviations from the Watson–Crick global average. The massive expansion and hypermethylation of the duplex triplet repeat $(CCG)_n(CGG)_n$ has characteristic higher-order structures that are associated with the fragile *X* syndrome. We have used luminescent mineral nanoparticles of protein-sized cadmium sulfide in optical assays to detect anomalous DNA structures. The photoluminescence of these particles is sensitive to the presence and nature of adsorbates. We previously found that our nanoparticles bind the fragile *X* repeat well but do not bind to normal double-helical DNA. In this study, we have determined that these particles are also able to detect the hypermethylated forms of these triplet repeats. Therefore, these nanoparticles may form the basis for future optical assays of higher-order DNA structures, especially those associated with human disease. *© 2001 Society of Photo-Optical Instrumentation Engineers.* [DOI: 10.1117/1.1344189]

Keywords: DNA; oligonucleotide; nanoparticle; quantum dot; photoluminescence; CdS.

Paper CARD-01 received May 16, 2000; accepted for publication Sep. 13, 2000.

1 Introduction

The canonical double-helical structure of B-form DNA is widely recognized. However, recent findings demonstrate that numerous, biologically significant, sequence-induced local structural deviations from this Watson–Crick global average are interspersed throughout the human genome.[1,2] For example, repetitive DNA sequences constitute ~30% of the human genome.[1] Single-stranded DNA can adopt unusual higher-order structure as well.[1–6] Several studies indicate that 5′-*d*$(CGG)_7$-3′ forms hairpins and tetraplexes (Figure 1),[7–10] whereas 5′-*d*$(CCG)_7$-3′ prefers hairpin formation.[1,2,7–10] These hairpin formations create C–C mismatches, which are prone to methylation at CpG islands *in vivo*.[1] The link of this hypermethylation with massive triplet repeat expansion at the 5′ untranslated region of the fragile *X* mental retardation type 1 (FMR-1) gene is correlated with fragile *X* syndrome.[1,2]

We have employed cadmium sulfide (CdS) semiconductor nanoparticles, 40–50 Å in diameter, as protein-sized photoluminescent probes of DNA structure.[11–15] The photoluminescence of CdS is heavily influenced by adsorbates, and we found that intrinsically ''kinked'' DNA binds more strongly and more quickly to the curved CdS surface than does ''straight'' DNA of the same nominal length.[11–15] Thus, DNA sequence, and by implication local DNA structure and/or flexibility, influences the binding of the DNA polymer to the nonspecific colloidal CdS.[11]

In the present paper, we examine the interactions of single-stranded hypermethylated triplet repeats (all cytosines 5-methylated) with our protein-sized cationic nanoparticles. We had previously found that nonmethylated triple repeat DNA structures could be optically detected by our nanoparticles.[11] Methylation might be expected to perturb not only the DNA structure, but also the counterion atmosphere and water solvation shell around the DNA,[16] and thus affect the interaction of our nanoparticle probes with these hypermethylated triplet repeat structures.

2 Experiment

2.1 Materials

Anhydrous Na_2S (Alfa), $Cd(NO_3)_2 \cdot 4H_2O$ (Aldrich), NaOH (Mallinckrodt), and sodium polyphosphate (average chain length of 18, Sigma) were used as received. Reagents for buffers were all of the highest purity available: Trizma (tris hydrochloride), EDTA dipotassium salt, KCl, triethylamine, and acetonitrile.

2.2 Synthesis of Materials

Syntheses of the oligonucleotides, 5′-*d*$(^mCGG)_7$-3′ and 5′-*d*$(^mC^mCG)_7$-3′, were accomplished by standard phosphoramidite methods at the University of South Carolina Institute for Biological Research and Technology's Oligonucleotide Synthesis Facility. Within each strand, every cytosine was methylated at the 5 position. Purification of the oligonucleotides was achieved by reverse-phase high pressure liquid chromatography (HPLC). The oligonucleotides were subsequently dissolved in tris-EDTA buffer (10 mM tris hydrochloride, 1 mM EDTA dipotassium salt, 200 mM KCl, pH 8.0). Aggregated structures were induced by annealing the oligonucleotides at 90 °C for 10 min, allowing them to cool to room temperature, and storing them at 4 °C for ~48 h. DNA concentrations were calculated using the measured absorbance at 260 nm and 90 °C and a weighted average of base extinction coefficients at 260 nm. The aggregated DNA

Address all correspondence to Catherine J. Murphy. Tel: 803-777-3628; Fax: 803-777-9521; E-mail: murphy@mail.chem.sc.edu

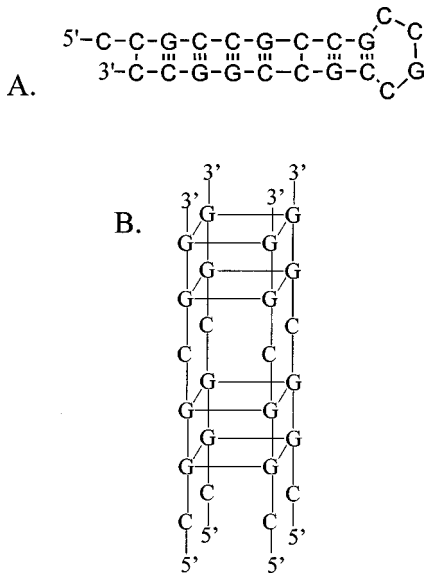

Fig. 1 Suggested higher-order structures of $d(^{m}C^{m}CG)_7$, a hairpin (A) and $d(^{m}CGG)_n$, a tetraplex (B).

structures were characterized by melting curves using absorbance spectroscopy and circular dichroism (CD) spectroscopy. The HPLC-purified oligonucleotide 5′-GGCAACCTGAGGACCC-3′ and its complement were used as received from Genemed. They were annealed as described above and served as a ''normal'' double-stranded DNA control. As we described in previous research, Cd(II)-activated CdS nanoparticles that were 45 Å in diameter and surface-enriched with Cd(II) were synthesized as a colloidal dispersion in water.[12] To characterize the nanoparticles, we used transmission electron microscopy (TEM) to confirm particle size, and absorption and photoluminescence spectroscopies.

2.3 Instrumentation

HPLC was performed on a Beckman Gold system with an ultraviolet/visible absorption detector module. A Hamilton PRP-1 reversed-phase HPLC column was used with an acetonitrile/triethylammonium acetate aqueous buffer (pH 7.0) gradient. Absorption spectra were obtained with a Varian Cary 500 Scan UV-Vis-near-infrared spectrophotometer. Photoluminescence spectra were determined using an SLM-Aminco 8100 spectrofluorometer, with excitation at 350 nm and a 4 nm band pass. CD spectra were obtained on an Olis 1600 instrument. TEM was performed on a Hitachi H-8000 instrument utilizing nitrocellulose grids.

2.4 Procedures

Photoluminescence titrations were performed by adding 5 μL aliquots of DNA (~1 mM nucleotide) to 400 μL of a 2×10^{-4} M (Cd) Cd(II)–CdS solution. Emission spectra were acquired 20 min after each DNA aliquot was added. This provided adequate time to ensure equilibrium was achieved.[13] Blank titrations of buffer, without DNA, were performed and used to correct the data for subsequent analysis.

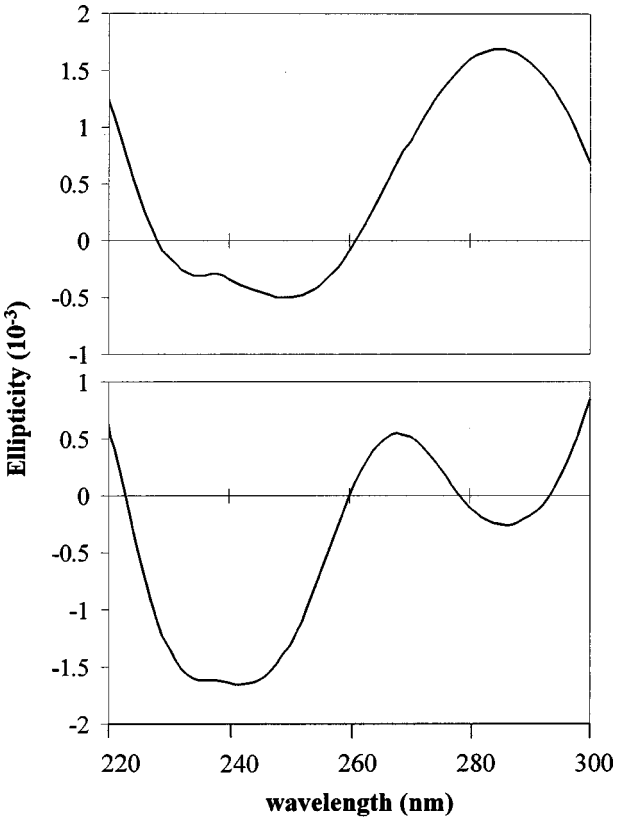

Fig. 2 Circular dichrosim spectra of $d(^{m}C^{m}CG)_7$ (top) and $d(^{m}CGG)_7$ (bottom).

3 Results

Figures 2 and 3 show the circular dichroism spectra and the melting temperature plots of $d(^{m}C^{m}CG)_7$ and $d(^{m}CGG)_7$. Both sets of data suggest the formation of stable, higher-order structures at room temperature. The literature predicts that $d(^{m}CGG)_7$ forms a tetraplex regardless of whether the cytosines are methylated.[7] The structure of $d(^{m}C^{m}CG)_7$ is not as well documented, but according to the CD studies of nonmethylated $d(CCG)_n$, $d(^{m}C^{m}CG)_7$ may form a hairpin-like structure.[7,11,17–19]

Figure 4 shows the emission spectra of Cd(II)-rich CdS nanoparticles without DNA and in the presence of equal molar concentrations of duplex $d(^{m}C^{m}CG)_7$, or $d(^{m}CGG)_7$ DNA. The presence of all three sequences contributed to photoluminescence quenching; however, the absolute change in photoluminescence was sequence dependent. Duplex or $d(^{m}CGG)_7$ DNA quenched the particle luminescence in nearly equal proportions, and $d(^{m}C^{m}CG)_7$ resulted in more photoluminescent (less quenched) nanoparticle solutions. Buffer alone, which contained 1 mM EDTA, also contributed to a large degree of quenching (~50%–70% of the maximum with DNA) due to the affinity of EDTA to complex with activating Cd^{2+} that produces the 460 nm emission band.[7–11]

We monitored the integrated intensity decrease of the 460 nm emission band with respect to DNA concentration (Figure 5) and fit the Frisch–Simha–Erich (FSE) isotherm, derived for a long polymer adsorbing in short segments to a locally

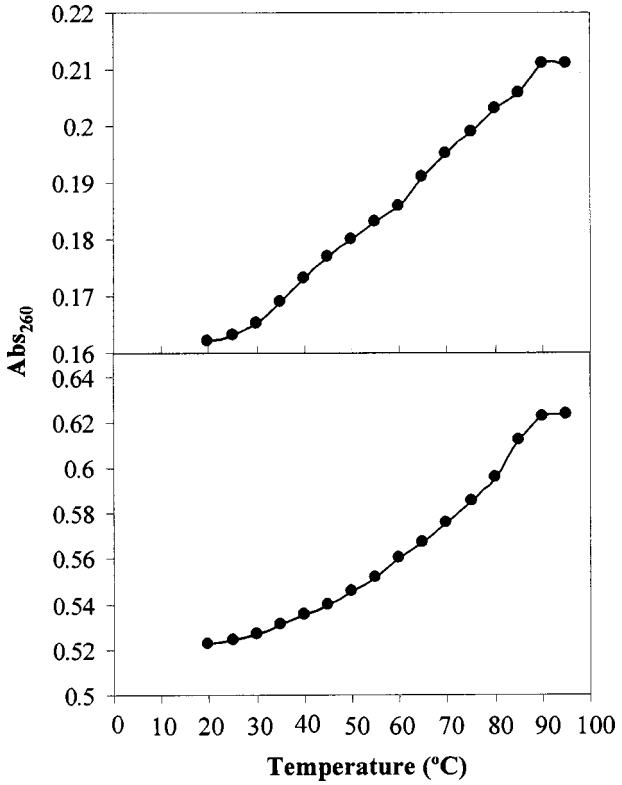

Fig. 3 Melting curves for $d(^{m}C^{m}CG)_7$ (top) and $d(^{m}CGG)_7$ (bottom).

flat surface,[20] to our data to obtain relative equilibrium binding constants (Figure 5):

$$[\theta \exp(2K_1\theta)]/(1-\theta) = (KC)^{1/\nu}, \quad (1)$$

where θ is the fractional surface coverage, which is assumed to be directly proportional to fractional change in luminescence intensity[11–15,21,22] and $\theta = (PL - PL_0)/(PL_f - PL_0)$, where PL is the intensity of photoluminescence at an arbitrary point in the titration, PL_0 is the initial photoluminescence intensity before DNA is added, and PL_f is the photoluminescence intensity at which no further changes take place as

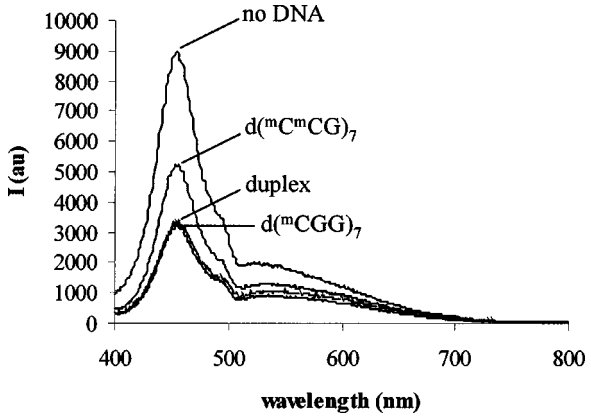

Fig. 4 Photoluminescence spectra of Cd(II)-rich CdS nanoparticles containing no DNA and after addition of 0.20 mM (per nucleotide) duplex DNA, $d(^{m}C^{m}CG)_7$, and $d(^{m}CGG)_7$ to separate equal-volume nanoparticle solutions.

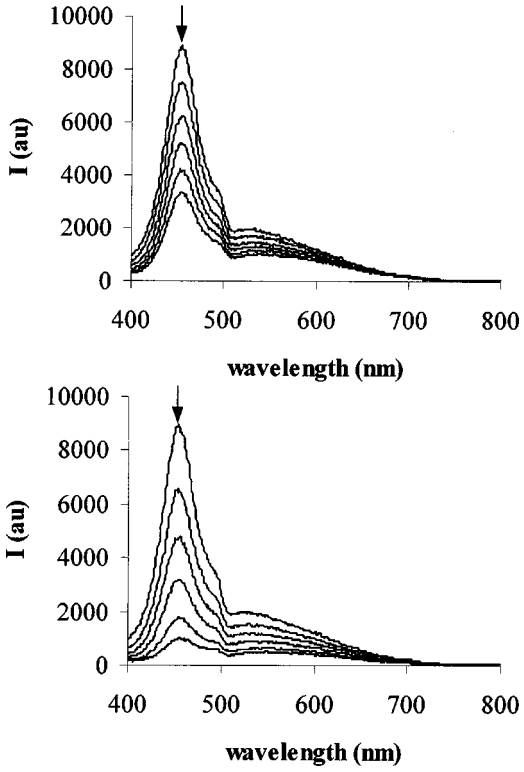

Fig. 5 Luminescence titrations of 400 μL Cd(II)-rich CdS nanoparticle solution with $d(^{m}C^{m}CG)_7$ (top) and $d(^{m}CGG)_7$ (bottom). In all cases CdS photoluminescence is decreased. DNA concentrations were 0.0, 0.067, 0.13, 0.20, 0.26, and 0.32 mM (per nucleotide) during the titrations.

DNA is added; C is the DNA concentration in molar nucleotides; K_1 is a constant that is a function of the interaction of adsorbed polymer segments and has empirically been found to give best fits when set to 0.5, as it is here;[12] K is the equilibrium binding constant; and ν is the average number of polymer segments attached to the surface, which has a nonobvious meaning in our system (since our polymers are very short and aggregated). Our definition of θ implicitly assumes a two-state model for the nanoparticle–DNA interaction; the nanoparticle is either bound to DNA (and emits with intensity $PL_0 - PL_f$ depending on DNA concentration), or free of DNA (and emits with intensity PL_0).

We have previously applied the FSE adsorption isotherm to luminescence data to understand the interactions among protein-sized CdS quantum-dot particles and other sequences of DNA.[11–15] In earlier work, we showed that unmethylated $d(CGG)_7$ and $d(CCG)_7$ perturb the photoluminescence of 45 Å Cd(II)–CdS nanoparticles under conditions where duplex DNA does not bind to the particles above the buffer background.[11] Relative binding constants for these DNAs, as judged by the FSE theory of polymer adsorption were 13 000 M^{-1} for $d(CGG)_7$ and 6100 M^{-1} for $d(CCG)_7$.[11] Competitive photoluminescence binding experiments confirmed this ordering.[11] Here, binding constants of 17 000 M^{-1} were calculated for both $d(^{m}C^{m}CG)_7$ and $d(^{m}CGG)_7$ DNA, while normal double-helical DNA bound with a K of 32 000 M^{-1}. This is the opposite of what we observe with the nonmethylated analogs of the triplet repeats.[11] Interestingly, compared

to all of our other studies, $d(^{m}C^{m}CG)_7$ is not capable of quenching all the photoluminescence from the 460 nm emission band of the nanoparticles (Figure 5). Thus, even though nanoparticle solutions containing $d(^{m}C^{m}CG)_7$ emit more intensely than those containing $d(^{m}CGG)_7$, the binding constants come out the same.

4 Discussion

Our results indicate that hypermethylated higher-order structures can be detected by protein-sized Cd(II)-rich CdS nanoparticles, although duplex DNA is a significant interferent. The FSE data suggest that there is no preferential binding of $d(^{m}C^{m}CG)_7$ compared to $d(^{m}CGG)_7$, but the differences in absolute photoluminescence imply a different interaction for each structure with the nanoparticle substrate. The mechanism of nanoparticle photoluminescence quenching is not entirely well understood, but since it is reversible with salt[15] and results in no permanent base damage after irradiation,[12] we think of the nanoparticle–DNA interaction as a simple donor–acceptor adduct, familiar from inorganic chemistry. The loss of the surface-associated Cd^{2+} is one likely source of quenching, and in fact studies with double-stranded DNA suggest that counterion release from the nanoparticle–DNA interface is the thermodynamic driving force for the interaction.[15] The salt dependence of the binding constants for long DNA to Cd(II)-rich CdS supports the notion that these nanoparticles are cationic in solution;[15] we have not yet investigated the interaction of CdS nanoparticles capped with other surface groups with these DNAs.

With these thoughts in mind, we can begin to interpret the interaction of the hypermethylated single-stranded structures with the cationic nanoparticle surface. One additional difficulty is that the structures of these sequences are not completely known. Evidence supports formation of a tetraplex for $d(^{m}CGG)_7$,[7–10] but there seems to be no consensus on the higher-order structure of $d(^{m}C^{m}CG)_7$.[7] However, electrophoretic gel mobility experiments show a fast moving band for a ^{m}C-rich strand, whereas the G-rich strand moves more slowly.[7] This result suggests that the C-rich strand would form a less bulky, possibly hairpin-like structure. CD spectra of the individual strands concur with findings that indicate that G- and C-rich strands form tetraplex and hairpin-like structures.[7–11]

If we imagine that both $d(^{m}CGG)_7$ and $d(^{m}C^{m}CG)_7$ ball up into somewhat rigid higher-order structures that do not wrap about the nanoparticle's curvature, then it is reasonable for their binding constants to the cationic nanoparticles to be similar, on a per-nucleotide basis. However, as noted above, $d(^{m}C^{m}CG)_7$ is not able to quench the emission to the extent that duplex DNA and $d(^{m}CGG)_7$ do. This may reflect differences in the surface area of the DNA–nanoparticle interface for these higher-order methylated structures. The DNA backbone surface area exposed to the Cd(II)-rich CdS nanoparticle may be greater for the G-rich structure than for the C-rich structure, which would expel more counterions from the nanoparticle surface and produce more photoluminescence quenching compared to the C-rich strand. Salt-dependent equilibrium binding studies are needed to sort out the possibilities. The DNAs may also differentially induce aggregation of the nanoparticles, which may be another parameter to include in understanding the system, which may be accessible by dynamic light scattering studies.[23–25] Nonetheless, the luminescent mineral nanoparticles we have described are a new kind of optical reporter for biological applications that may fruitfully be explored for other diagnostic assays.

References

1. P. Catasti, X. Chen, S. V. S. Mariappan, E. M. Bradbury, and G. Gupta, ''DNA repeats in the human genome,'' *Genetica (The Hague)* **106**, 15–36 (1999).
2. X. Chen, S. V. S. Mariappan, P. Catasti, R. Ratliff, R. K. Moyzis, A. Laayoun, S. S. Smith, E. M. Bradbury, and G. Gupta, ''Hairpins are formed by the single DNA strands of the fragile X triplet repeats: Structure and biological implications,'' *Proc. Natl. Acad. Sci. U.S.A.* **92**, 5199–5203 (1995).
3. *Unusual DNA Structures*, R. D. Wells and S. C. Harvey, Eds., Springer, New York (1988).
4. R. R. Sinden, *DNA Structure and Function*, Academic, San Diego, CA (1994).
5. A. P. Wolffe and H. R. Drew, ''DNA structure: implications for chromatin structure and function,'' in *Chromatin Structure and Gene Expression*, S. C. R. Elgin, Ed., pp. 27–48, IRL, Oxford (1995).
6. C. R. Calladine and H. R. Drew, *Understanding DNA*, Academic, San Diego, CA (1997).
7. M. Fry and L. A. Loeb, ''The fragile *X* syndrome $d(CGG)n$ nucleotide repeats form a stable tetrahelical structure,'' *Proc. Natl. Acad. Sci. U.S.A.* **91**, 4950–4954 (1994).
8. M. X. Zheng, X. N. Huang, G. K. Smith, X. Y. Yang, and X. L. Gao, ''Genetically unstable CXG repeats are structurally dynamic and have a high propensity for folding. An NMR and UV spectroscopic study,'' *J. Mol. Biol.* **264**, 323–336 (1996).
9. J. M. Darlow and D. R. F. Leach, ''Secondary structures in $d(CGG)$ and $d(CCG)$ repeat tracts,'' *J. Mol. Biol.* **275**, 3–16 (1998).
10. J. M. Darlow and D. R. F. Leach, ''Evidence for two preferred hairpin folding patterns in $d(CGG)d(CCG)$ repeat tracts *in vivo*,'' *J. Mol. Biol.* **275**, 17–23 (1998).
11. C. J. Murphy and R. Mahtab, ''Detection of unusual DNA structures with nanoparticles,'' *Proc. SPIE* **3924**, 10–16 (2000).
12. R. Mahtab, J. P. Rogers, and C. J. Murphy, ''Protein-sized quantum dot luminescence can distinguish between 'straight,' 'bent,' and 'kinked' oligonucleotides,'' *J. Am. Chem. Soc.* **117**, 9099–9100 (1995).
13. R. Mahtab, J. P. Rogers, C. P. Singleton, and C. J. Murphy, ''Preferential adsorption of a 'kinked' DNA to a neutral curved surface: Comparisons to and implications for nonspecific DNA-protein interactions,'' *J. Am. Chem. Soc.* **118**, 7028–7032 (1996).
14. C. J. Murphy, E. B. Brauns, and L. Gearheart, ''Quantum dots as inorganic DNA-binding proteins,'' *Mater. Res. Soc. Symp. Proc.* **452**, 597–600 (1997).
15. R. Mahtab, H. H. Harden, and C. J. Murphy, ''Temperature- and salt-dependent binding of long DNA to protein-sized quantum dots: Thermodynamics of 'inorganic protein'-DNA interactions,'' *J. Am. Chem. Soc.* **122**, 14–17 (2000).
16. C. Mayer-Jung, D. Moras, and Y. Timsit, ''Hydration and recognition of methylated CpG steps in DNA,'' *EMBO J.* **17**, 2709–2718 (1998).
17. A. Yu, M. D. Barron, R. M. Romero, M. Christy, B. Gold, J. Dai, D. M. Gray, I. S. Haworth, and M. Mitas, ''At physiological pH, $d(CCG)_{15}$ forms a hairpin containing protonated cytosines and a distorted helix,'' *Biochemistry* **36**, 3687–3699 (1997).
18. P. Balagurumoorthy, S. K. Brahmachari, D. Mohanty, M. Bansal, and V. Sasisekharan, ''Hairpin and parallel quartet structures for telomeric sequences,'' *Nucleic Acids Res.* **20**, 4061–4067 (1992).
19. F. M. Chen, ''Acid-facilitated supramolecular assembly of G-quadruplexes in $d(CGG)_4$,'' *J. Biol. Chem.* **270**, 23090–23096 (1995).
20. R. Simha, H. L. Frisch, and F. R. Eirich, ''The adsorption of flexible macromolecules,'' *J. Phys. Chem.* **57**, 584–589 (1953).
21. C. J. Murphy, G. C. Lisensky, L. K. Leung, G. R. Kowach, and A. B. Ellis, ''Photoluminescence-based correlation of semiconductor depletion widths with adsorbate Hammett substituent constants. Adsorption of aniline derivatives on cadmium selenide,'' *J. Am. Chem. Soc.* **112**, 8344–8348 (1990).

22. R. Cohen, L. Kronik, A. Shanzer, D. Cahen, A. Liu, Y. Rosenwaks, J. K. Lorenz, and A. B. Ellis, ''Molecular control over semiconductor surface electronic properties: dicarboxylic acids on CdTe, CdSe, GaAs and InP,'' *J. Am. Chem. Soc.* **121**, 10545–10553 (1999).
23. K. Sooklal, L. H. Hanus, H. J. Ploehn, and C. J. Murphy, ''A blue emitting CdS-dendrimer nanocomposite,'' *Adv. Mater.* **10**, 1083–1087 (1998).
24. J. Huang, K. Sooklal, C. J. Murphy and H. J. Ploehn, ''Polyamine-quantum dot nanocomposites: linear versus starburst stabilizer architectures,'' *Chem. Mater.* **11**, 3595–3601 (1999).
25. L. H. Hanus, K. Sooklal, C. J. Murphy and H. J. Ploehn, ''Aggregation kinetics of dendrimer-stabilized CdS nanoclusters,'' *Langmuir* **16**, 2621–2626 (2000).